Manuscript for publication as *Research Paper* in *Industrial Crops and Products*

Tannin Microcapsules for Synergy-Enhanced Sunscreen Formulations

Elisabetta Alfonsi[a], Heiko Lange [b,c,†,*], and Claudia Crestini [c,d,†,*]

a University of Rome 'Tor Vergata', Department of Chemical Science and Technologies, Via della Ricerca Scientifica, 00133 Rome, Italy

b University of Milano-Bicocca, Department of Earth and Environmental Sciences, Piazza della Scienza, 20126 Milan, Italy

c CSGI - Center for Colloid and Surface Science, Via della Lastruccia 3, 50019 Sesto Fiorentino, Italy

d 'Ca' Foscari' University of Venice, Department of Molecular Sciences and Nanosystems, Via Torino 155, 30170 Venice Mestre, Italy

† Affiliated with a) *via* NAST – Nanoscience & Nanotechnology & Innovative Instrumentation Center.

* Corresponding authors: heiko.lange@unimib.it
claudia.crestini@unive.it

Highlights

- Sunscreen agents were encapsulated by a ultrasound technique in tannin microcapsules.
- Release kinetics of TMCs have been studied mimicking skin conditions.
- A synergistic effect by the tannin and the controlled active release was observed.
- A sustainable and environmentally benign UV-protection system has been developed.

Abstract

Salicylate and benzoate sunscreen agents have been encapsulated by the green, fast and robust ultrasound technique in tannin microcapsules (TMCs). The generated TMCs, obtained without use of cross linking agents, were fully characterised, including encapsulation efficiencies with respect to the encapsulated actives. Release kinetics of TMCs have been studied mimicking skin conditions. Body cream base samples containing specific concentrations of microcapsules filled with sunscreen actives were prepared and showed synergistic effects in terms of UV-protection abilities generated by the interplay between sunscreen actives and natural tannin polyphenols. The synergistic effect exerted by the tannin and the controlled active release allows to reduce the amount of synthetic sunscreens needed, and does thus contribute to the development of more sustainable and environmentally benign UV-protection systems.

Keywords

tannins, sunscreens, microcapsules, UV spectroscopy, transmittance, synergy

1. Introduction

Elevated exposure to ultraviolet radiations causes skin problems as burns and dermatitis and poses risks over time as the development of skin cancer becomes more probable due to irreversible damages (Ichihashi et al., 2003; Pfeifer, 2020; Soehnge et al., 1997). The UV spectrum includes UV-A radiations between 290 and 320 nm, the most responsible for immediate tanning, ageing and suppression of immunologic function, and UV-B radiations between 320 and 400 nm, which are responsible of sunburns and considered the leading risk factor for melanoma skin cancer. Application of topical sunscreens containing various countermeasures to UV irradiation is essential to provide protection against skin damages. Several sunscreen products are present on the market, grouped in physical and chemical sunscreens according to their modes of actions and corresponding formulation. While physical sunscreens rely on reflection properties of inorganic molecules (Pal et al., 2020; Masui et al., 2006; Lapidot et al., 2003; More, 2007; Kollias, 1999; Jiménez Reinosa et al., 2016), the chemical sunscreens are active regarding the absorption of specific wavelengths of UV radiation for protecting the cells of the epidermis (Burnett and Wang, 2011; Donglikar et al., 2016; Gasparro et al., 1998; Patel et al., 1992). Among the most frequently used chemical sunscreens are: i) cinnamates, *para*-aminobenzoate (PABA) derivatives, salicylates, benzophenones, camphor derivatives, dibenzoyl methanes, and anthranilates. Cinnamates, PABA derivatives, salicylates and camphor derivatives are all mainly UV-B absorbers, while benzophenone derivatives, dibenzoyl methanes and anthranilates are mainly UV-A absorbers (Gasparro et al., 1998). However, commercial sunscreens are unable to give a complete sunscreen protection and have a limited duration of action. Moreover, the synthetic chemicals contained in these products can cause unexpected side effects on skin, especially upon long-term application (Burnett and Wang, 2011; Gasparro et al., 1998; Kim and Choi, 2014; Petersen and Wulf, 2014; Scheuer and Warshaw, 2006; Suh et al., 2020), as well as environmental pollution caused by mass production and increased use (Kim and Choi, 2014; Narla and W. Lim, 2020; Sánchez-Quiles et al., 2020; Schneider and Lim, 2019).

The cosmetic industry can face these restrictions by turning its attention to natural extracts (Gordobil et al., 2020). in particular, polyphenols in form of lignins and tannins, which are natural products that can be found in most of the higher plants on Earth (Pizzi, 2008; Khanbabaee and Ree, 2001; Vanholme et al., 2010), held always promising characteristics for a use in sunscreens (Urbach, 2001). Nevertheless, lignins were more often exploited in recent studies on novel sunscreen applications (Ibrahim et al., 2019; Lee et al., 2020, 2019; Li et al., 2019; Qian et al., 2017, 2014; Qiu et al., 2018; Zhang et al., 2019, 2018); their widespread use, however, is problematic due to lignin-inherent peculiarities, such as colour, eventual irritating nature as reminiscence of the isolation process, etc. Tannins offer a much better class of polyphenols in this context. Beside their UV absorbing properties, the significant antioxidant and radical scavaging characteristics of tannins make them interesting cosmetics components with possible skin preserving and antiwrinkle activity. Furthermore, tannins display significant natural anti-inflammatory activity (Pizzi, 2008; Thomas and Filho, 1985) that is definitely an added value in situations where the skin is subject to external stresses.

Tannins are oligo- or polymeric polyphenols produced in almost all parts of the plant as a defence against insects, fungi and bacteria (Pizzi, 2008). With respect to the structure-related chemical characteristics, two classes of tannins are identified: hydrolysable and condensed tannins (Mueller-Harvey, 2001). While the first class of tannins is comprised of polyphenols that are soluble and hydrolysable into their components in alkaline solutions, the second class comprises are oligomers and polymers of different flavan-3-ol units, linked by C-C bonds not susceptible to hydrolytic cleavage. They can, however, be decomposed to anthocyanidins by acid-catalysed oxidation reactions. Addition of a third phenolic group on the B-ring yields gallocatechin- and epigallocatechin derivatives (GC) (Figure 1). The different B-ring hydroxylation patterns of the major subunits of flavan-3-ols are either 3,4-dihydroxyphenyl (catechol hydroxylation pattern) or 3,4,5-trihydroxyphenyl (pyrogallol hydroxylation pattern) and, for the A-ring, 7-hydroxyphenyl (resorcinol hydroxylation pattern) or 5,7-dihydroxyphenyl (phloroglucinol hydroxylation pattern),

determining the complexing and biological properties of different condensed tannins. *Schinopsis balansae* wood extract, as well as *Acacia mearnsii* bark extract, are condensed tannins whose structure (Crestini et al., 2016; Zhen et al., 2021) and biological activities render them suitable for the purposes of the present study. Rather than replacing synthetic sunscreen actives with biomolecules, it is more promising to boost the activities mutually such as to be able to reduce overall amount of the substances and/or to extend their efficacy, generating eventually synergistic effects adding new features to sunscreen formulations.

The combination of synthetic UV screens with natural products such as tannins, would lead *per se* to an upgrading of cosmetic features thanks to the antioxidant, anti-inflammatory and antibacterial properties of the tannin (Pizzi, 2008). However, a mere mixing together of synthetic and natural active ingredients does not represent the full exploitation potential. In the present effort, commercial UV screens have been entrapped into suitably designed and developed natural tannins microparticles for synergy enhanced active controlled release. Combining synthetic and natural actives in form of micro- and nanostructures offers additional benefits by introducing a third aspect of improved action beyond a broader activity profiles and synergy: nano- and microtechnology offers a timing component via tunable release kinetics.

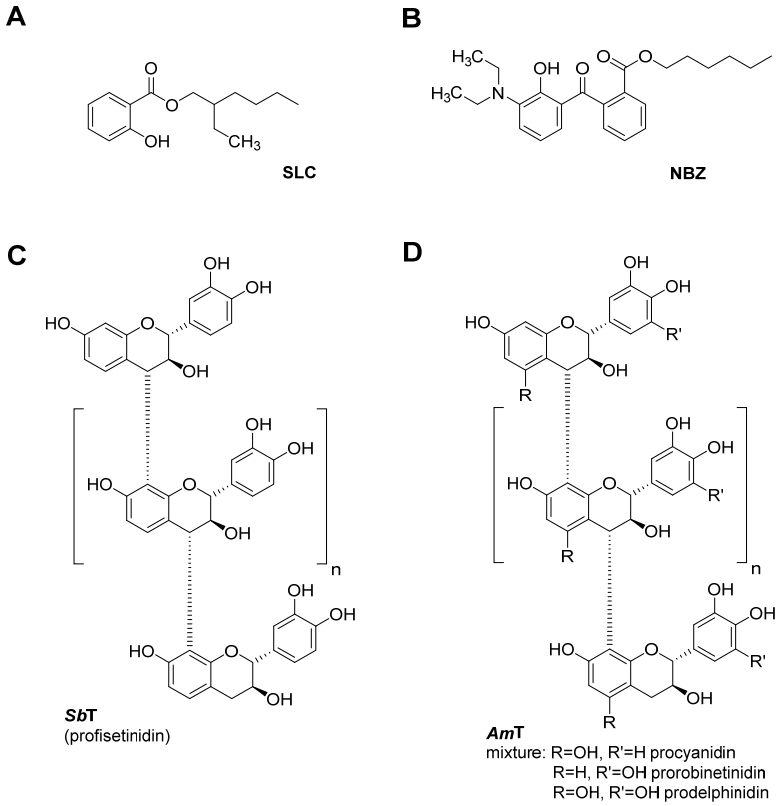

Figure 1. Synthetic sunscreen actives and condensed tannins used for synergy-enhanced sunscreen applications: (A) UV-A-targeting hexyl-2-[3-(diethylamino)-2-hydroxybenzoyl] benzoate (**BNZ**); (B) UV-B-targeting 2-ethylhexyl salicylate (**SLC**); (C) *Schinopsis balansae* wood extract tannin (***Sb*T**) and (D) *Acacia mearnsii* bark extract tannin (***Am*T**). The structural characterization of the two tannin species was delineated as described elsewhere.(Crestini et al., 2016)

The present study demonstrates the ultrasound-mediated encapsulation of synthetic sunscreen actives, *i.e.*, UV-A-targeting hexyl-2-[3-(diethylamino)-2-hydroxybenzoyl] benzoate (**BNZ**) and UV-B-targeting 2-ethylhexyl salicylate (**SLC**), into microcapsules of oligomeric condensed tannins from *Schinopsis balansae* wood (***Sb*T**) and *Acacia mearnsii* bark (***Am*T**), respectively (Figure 1) (Bartzoka et al., 2017). It further investigates the synergistic potential of the newly generated sunscreen systems in body cream matrices and the active release kinetics.

2. Materials and methods

2.1. General information

Solvents and chemicals, including buffer salts, were purchased from Sigma-Aldrich in appropriate grades, and were used without further purification if not stated otherwise. *Schinopsis balansae* wood extract (***Sb*T**) and *Acacia mearnsii* bark extract (***Am*T**) were obtained from Figli di Guido Lapi. The sunscreen actives 2-ethylhexyl salicylate (**SLC**) and hexyl-2-[3-(diethylamino)-2-hydroxybenzoyl] benzoate (**BNZ**)**,** as well as refined olive oil and linoleic acid were obtained from Sigma Aldrich. Glyceryl stearate was purchased from Alfa Aesar and Cocoa butter was bought in a common local pharmacy.

*2.2. Generation of **SbT** and **AmT** microcapsules by ultrasound sonication*

Previously published procedures were adopted for this study (Bartzoka et al., 2017). *Tannin component solution:* ***Sb*T** and ***Am*T** solutions were prepared by dissolving 50 mg of respective tannin in 10 ml of 0.1 M MOPS buffer at pH = 7.35, obtaining a concentration of 5 mg/ml.

Synthetic sunscreen components solution: i) **SLC** was dissolved in olive oil spiked with linoleic acid (5% (v/v)), at a concentration of 1 mg/ml. The solution was left stirring for 1h. ii) 0.1 g of **BNZ** were dissolved in 0.6 g of neat **SLC** in a 1:6 (m/m) ratio, and the mixture was stirred until all the **BNZ** was dissolved.

Capsule formation: four types of samples were prepared using various 1/1 combinations of aqueous and oily phase, starting for each with 500 μl of aqueous tannin solution, adding i) 500 μl of olive oil, ii) 500 μl of **SLC** in olive oil at various concentrations, iii) 500 μl of pure **SLC**, and iv) 500 μl of 15% (w/w) **BNZ** in pure **SLC**. Samples were sonicated using a Branson Digital Sonifier Model 450L (Ultrasonic Corporation) equipped with a 20 kHz Branson probe ending in a sonication tip at room temperature (RT) with a power of 160 W (40% amplitude) for selected amounts of time. Obtained emulsions were centrifuged at 5000 rpm for 15 min, leading to the separation of a foamy layer of capsules from the aqueous phase. The capsules were washed with 1 ml of distilled water,

vortexed to bring them in suspension and centrifuged at the same conditions as mentioned above. This process was performed three times; after the third round, capsules were isolated and stored in the dark. TMCs were characterized determining statistical key data using optical microscopy.

2.3. Preparation of body cream base

Following available literature (Jiménez Reinosa et al., 2016), 50 g of cream base were prepared, according to the formulation reported in Table 1. The fatty phase ingredients were melted in a water bath at 60-70 °C. At the same time, the ingredients of the aqueous phase were heated at the same conditions and left under stirring. Once the melting temperature was reached, the fatty phase was added to the aqueous phase under constant stirring to form a stable emulsion that was allowed to slowly cool down to RT.

Table 1. Ingredients of body cream base.(Jiménez Reinosa et al., 2016)

component	ingredients	% weight
fatty phase	Lanolin	4.5
	Cocoa butter	2.0
	Glyceryl Stearate	3.0
	Stearic acid	2.0
aqueous phase	Water	72.0
	Sorbitol	5.0
	Triethanolamine	1.0
	Benzyl alcohol	0.5

2.4. Preparation of TMC-containing body cream

1 g of cream was prepared in a dark glass vial, by mixing 10% (w/w) of freshly prepared ***Sb*T** MCs containing **SLC** in olive oil with the base cream. The same procedure has been followed to prepare cream samples containing **S*b*T** MCs containing neat **SLC** or **BNZ** dissolved in neat **SLC**. The samples were vortexed so that the capsules were homogeneously distributed in the cream medium. Capsule integrity was confirmed by optical microscope analysis.

2.5. Optical microscopy analysis and statistical analysis

Analysis was performed using an established procedure (Bartzoka et al., 2017): *Sample preparation:* 10 μL of the generated 'concentrated' **TMCs** were added in 990 μL of distilled H_2O to form a suspension of **TMCs**. 5 μL of this suspension were transferred on a microscope carrier glass slide and covered with a coverslip prior to microscopy analysis. In case the capsules significantly overlap, the sample should be further diluted, prior to analysis.

Analysis: A Zeiss Axio Scope A1 microscope was used for the image analysis. All images were obtained with 100 x objective lens magnification. For optimising the exploitation of the 100 x lens, a drop of mineral oil was placed on the coverslip prior the analysis to function as an optical bridge.

Processing: The pictures from the microscope were processed by using the image analysis software ImageJ in combination with a Microsoft Office Excel based analyses as described in great detail before. Average errors for the diameter and the number of **MCs** per millilitre of 0.08 μm and 0.17 10^{12} **MCs** / mL, respectively, were estimated.

2.6. Quantitative UV spectrophotometric analysis

Analysis was performed using a described procedure (Qian et al., 2014): *General UV-vis characterisations:* UV analysis was performed to identify/confirm λ_{max} of each sunscreen active and tannin between 250 and 800 nm in aqueous solution in 0.1 M MOPS buffer with 2% (v/v) heptaethoxy laurate: λ_{max}(**SLC**) = 308.0 nm, λ_{max}(**BNZ**) = 353.5 nm and λ_{max}(***Sb*T**) = λ_{max}(***Am*T**) = 281.5 nm. Sunscreen actives showed practically unchanged λ_{max} in ethyl acetate and hexane.

Calibration of UV Spectrophotometer for quantifying SLC contents: a 2 mg/ml standard solution was prepared by dissolving 20 mg of **SLC** in 10 ml of UV-grade ethyl acetate. A second standard solution was prepared by dissolving 20 mg of **SLC** in 10 ml of HPLC-grade hexane. The two calibration curves were built using serial dilutions of the mother solution.

Direct loading studies: 100 µl of capsules were placed in an Eppendorf tube, washed once with 500 µl of hexane and centrifuged at 5000 rpm for 5 min. The capsules were then washed with ethyl acetate, vortexed and immersed in ultrasonic bath for 15 min to disassemble them. The organic phase was withdrawn and fresh solvent was added. The process was repeated until all the capsules were dissolved. After each washing, the organic phases were combined and left under the fume-hood for the solvent to evaporate. The resulting solids were re-dissolved with 1.5 ml of ethyl acetate and each sample was sonicated for 15 min to facilitate dissolution. The amount of **SLC** was quantified based on the calibration curve that was constructed with **SLC** in ethyl acetate as described above.

Release studies: 100 µl of capsules were placed in an Eppendorf tube, one sample for each kind of ***Sb*T** capsule. 1 ml of acetate buffer 0.1 M at pH = 5.4 was added to each capsule sample, and the suspension was left under gentle agitation. After defined time intervals, the capsules were centrifuged at 5000 rpm for 5 min and the aqueous phase aliquot was withdrawn. In the case of **S*b*T** capsules containing pure **SLC** and **S*b*T** capsules containing **BNZ**/pure **SLC**, 0.5 ml of hexane were added before centrifugation and aliquots of both the organic and aqueous phases were withdrawn. Then, 1 ml of fresh acetate buffer was added to the remaining capsules, which were placed again under agitation. Universal time intervals for sampling were 30 min, 1 h, 2 h, 4 h, 8 h, 24 h and 48 h. The aqueous aliquots obtained from **S*b*T** capsules containing **SLC** in olive oil were freeze-dried, and residues re-suspended for analysis in 1.5 ml of ethyl acetate and centrifuged to remove the salts coming from the acetate buffer. In the case of TMC containing pure **SLC** and **BNZ**/pure **SLC**, the organic phase was used for the analysis. The amount of released **SLC** was quantified based on the calibration curves that were constructed as described above.

UV transmittance measurements of body cream base preparations: 25.4 mm x 25.4 mm x 1 mm quartz slides were covered entirely with 3M Transpore tape of 6.45 cm^2. For each cream sample, a minimum of three slides were prepared for the UV transmittance analysis; a reference slide was also prepared applying just pure cream base. MCs-containing cream was homogeneously

distributed across the pores of the tape, and any excess was removed before measurements. The samples were then placed in a dark room to dry for 20 min prior to the UV analysis.

3. Results and discussion

3.1. Encapsulation of sunscreen actives in tannin-based microcapsules by ultrasound sonication

Sunscreen active-filled TMCs were generated using conditions previously found to reliably deliver TMCs *via* the sonication method (Bartzoka et al., 2017), *i.e.*, mixing tannin solution (5 mg/ml) with the oily component in a 1:1 ratio and sonicating the emulsion for a defined amount of time at ambient temperature. Using ***Sb*T**, three sunscreen systems in form of four TMC samples were prepared for further studies: i) a control system with TMCs containing just olive oil; ii) a system for extended UV-B protection in form of TMCs filled with a) olive oil and **SLC**, and b) pure **SLC**; and iii) a system for combined UV-A and UV-B protection enhanced by tannin presence in the form of TMCs containing an olive oil-free **SLC**/**BNZ** mixture. ***Am*T** was used additionally to ***Sb*T** to demonstrate generality of the encapsulation of sunscreen actives in tannin MCs. With exception of the systems in which neat synthetic sunscreens were used as oily phase, systems were sonicated for both 1 and 10 minutes, to test for eventual effects in terms of encapsulation and release of actives. Isolated capsules were statistically analysed based on optical microscope images as reported before; Figure 2 shows capsules generated upon 1 minute of sonication, pictures of capsules obtained by sonicating for 10 min are given in Figure S1 in the Supplementary Data. Results are summarised in Table 2.

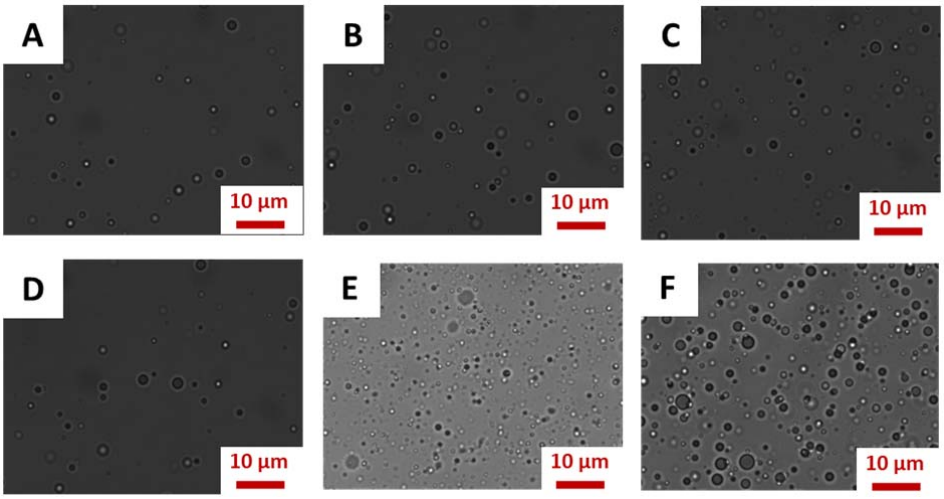

Figure 2. Optical micrographs of synthetic sunscreen-filled **TMCs** after 1 min of sonication: (A) **SLC**-filled ***Sb*T** MCs; (B) **BNZ**-filled ***Sb*T** MCs; (C) **SLC**-filled ***Am*T** MCs; (D) **BNZ**-filled ***Am*T** MCs; (E) **SLC**-filled ***Sb*T** MCs; (F) **BNZ/SLB**-filled ***Sb*T** MCs.

Table 2. Characterising statistical key data, yields, encapsulation efficiencies and 48 h release of sunscreen-containing **TMC** systems.

entry	tannin shell	core material	son. time [min]	mean Ø [µm]	PD	10^9TMCs / mL	EE [%]	48 h release [%]
1	***Sb*T**	**---**	1	2.53±1.15	0.38	113	---	---
2	***Sb*T**	**---**	10	2.43±0.69	0.22	183	---	---
3	***Sb*T**	**SLC** (0.1% (w/w) in O.O.)	1	2.24±0.81	0.30	79	68	11
4	***Sb*T**	**SLC** (0.1% (w/w) in O.O.)	10	1.93±0.72	0.32	132	37	19
5	***Sb*T**	**BNZ** (0.1% (w/w) in O.O.)	1	2.33±0.72	0.23	88	39	41
6	***Sb*T**	**BNZ** (0.1% (w/w) in O.O.)	10	2.23±0.77	0.28	140	27	93
7	***Sb*T**	**SLC** (50% (w/w) in O.O.)	1	1.90±0.75	0.32	201	n.d.	n.d.
8	***Sb*T**	**SLC** (neat)	1	1.74±0.82	0.22	157	n.d.	n.d.
9	***Sb*T**	**BNZ** (15% (w/w)) in **SLC** (neat)	1	1.86±0.75	0.33	148	n.d.	n.d.
10	***Am*T**	**SLC** (0.1% (w/w) in O.O.)	1	2.05±0.79	0.33	194	76	17
11	***Am*T**	**SLC** (0.1% (w/w) in O.O.)	10	1.93±0.88	0.46	147	41	13
12	***Am*T**	**BNZ** (0.1% (w/w) in O.O.)	1	2.10±0.66	0.26	108	35	51
13	***Am*T**	**BNZ** (0.1% (w/w) in O.O.)	10	2.13±0.82	0.31	106	18	44

The procedure for the synthesis of tannins microcapsules has shown to be quite robust: as expected, the **TMC** systems generated in the present effort exhibit, across the board, characterising statistical data that are similar to data obtained before for various types of filled and unfilled tannin microcapsules on the basis of the two condensed tannins used here (Bartzoka et al., 2017). Independent of the concentrations and the eventual mixing of synthetic sunscreen actives, microcapsule yields were around 100-200 10^9 TMCs/mL in concentrated form, with mean capsule diameters of around 2 μm. Longer sonication times led to slightly increased capsule yields, but did not significantly affect their size. Invariant sizes and yields obtained for ***Sb*-TMCs** containing undiluted sunscreens indicate that neat **SLC** can effectively be used as 'oily' phase itself, and as such even acting as 'solvent' for **BNZ** for the generation of TMCs. Importantly, optical microscope images (Figure 3) do suggest that the fundamental capsule nature is preserved in these cases; a mixing of tannins and sunscreen actives that would eventually lead to nanoparticle formation does not happen in the investigated combinations.

Efficiency of encapsulation was determined using a direct method. Following procedures established in our group using various polyphenol capsule systems (Bartzoka et al., 2018, 2017, 2016; Piombino et al., 2020), an aliquot of each type of sunscreen TMC system, typically 100 μl, was washed with hexane to eliminate eventual sunscreen active molecules stuck on the surface prior to disassembly, which was effectuated by ethyl acetate. While such eventual surface bound synthetic sunscreen molecules do not interfere with the intended synergistic and improved mode of action, it does slightly corroborate accurate direct determination of the encapsulation efficiency. Encapsulation efficiencies (EEs) for the sunscreen-containing TMC systems of around 20-80 % are found, with a strong dependence on the type of hydrophobic active and the sonication time.

Most noteworthy, good encapsulation efficiencies were found also for the systems containing neat synthetic sunscreen. Together with the statistical data, this further confirms that TMC formation is robust, as long as the oily phase allows for an effective biphasic system in the

presence of water so, that the tannins can effectively accumulate at the phase interphase for efficient electronic molecular interaction. Generally, a more efficient encapsulation of **SLC** is evident, thus suggesting a greater compatibility with the base olive oil-tannin MC system. Looking at log*P* values of **SLC** and **BNZ**, this observation is counter intuitive as log*P*(**BNZ**) is slightly higher. Obviously, logP is not a predictive value with respect to the eventual success of encapsulation, but electronic effects causing hydrophobic interactions and interactions between the aromatic systems present in tannins, olive oil components and the sunscreen actives would have to be considered.

3.2. Release kinetics of sunscreen actives from TMCs

Characterization of sunscreen active-filled tannin MCs was concluded by determining their release kinetics. Aiming to mimic skin surface conditions, release was studied in 0.1 M acetate buffer at pH 5.4. Established procedures applied before to polyphenol microcapsules were applied for these studies as detailed in the Experimental Methods (Bartzoka et al., 2018, 2017, 2016; Piombino et al., 2020). Figure 3 shows the different release profiles of capsules generated by 1 minute of sonication; practically identical release profiles of capsules generated upon 10 minutes of sonication are shown in Figure S2 in the Supplementary Data. Total released amounts after 48 h are given in Table 2.

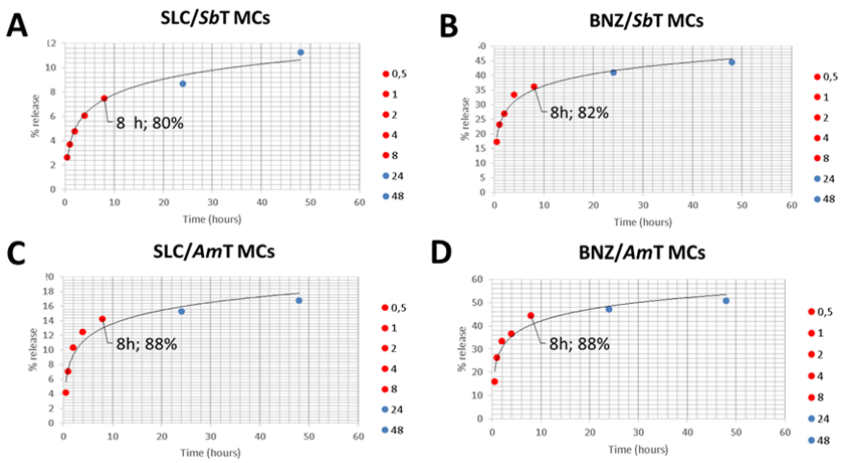

Figure 3. Release profiles for synthetic sunscreen-filled **TMCs** after 1 min of sonication: (A) **SLC**-filled ***Sb*T** MCs; (B) **BNZ**-filled ***Sb*T** MCs**;** (C) **SLC**-filled ***Am*T** MCs; (D) **BNZ**-filled ***Am*T** MCs.

In all cases more than 80% of the encapsulated active is out of the capsules in a time frame of 8h. After this time the release slows down significantly, reaching essentially full release plateaus after a two-day period. The overall release follows a first order kinetics, as it has been observed earlier in polyphenol microcapsule characterisations using identical set-ups for determining release (Bartzoka et al., 2018, 2017, 2016; Piombino et al., 2020). Release data reported in Table 2 do not reveal a common trend that would allow interpretation of release kinetics as function of sonication time. This suggests that higher sonication times do not drastically change shell thickness or shell stability in the system under study. Clearly visible, on the other hand, is the more effective release of **BNZ** over **SLB**, a finding that is in accordance with the observations made for the encapsulation efficiencies.

3.3. UV transmittance measurements of cream preparations

The main objective of this work was to evaluate a possible synergy in the sunscreen effect of actives and tannins in a real case scenario. To this end, sunscreen active-filled TMCs were mixed into a body cream base that was prepared following the recommended formulation from the

European Cosmetics Association (COLIPA) as indicated in Table 1 (Jiménez Reinosa et al., 2016). For control purposes, cream preparations were devised comprising: i) only olive oil (O.O.); ii) only ***Sb*T**; iii) only **SLC**; iv) simple mixes of **BNZ** and **SLC** or ***Sb*T** and **SLC**; v) ***Sb*T-MCs** containing just olive oil. Realised systems, kept in dark glass vials to protect the sunscreen formulation from sunlight, are summarised in Table 3.

Before measuring any sunscreen activity, optical and fluorescent microscopy analyses were conducted on various cream preparations containing sunscreen active-filled TMCS after two weeks of preparation, in order to test for the stability of TMCs in the cream matrix. Representative images are shown in Figure S1 in the Supplementary Data. Capsules exhibit a rather perfect stability in the cream base medium. These findings are in line with previous studies showing that polyphenol-based capsules suffer in acidic pH conditions and environments with high salinity, conditions that are absent in the cream matrix. Following a functional literature protocol for UV transmission measurements of cream preparations (Qian et al., 2014). sunscreen-TMC-containing cream and its controls were applied on quartz slides covered with 3M Transpore tape for analyses against a reference slide prepared using the cream base only. Figure S4 summarises the preparation process for the transmission measurements; Figure S5 shows an overview of the transmittance spectra obtained for the systems listed in Table 3 and diversely represented in Figure 4.

Table 3. Transmission spectroscopy data for different sunscreen-containing cream preparations and control systems. Capsules were generated by sonicating the mixtures for 1 min. samples were stored in the dark. The error in transmission is estimated to be ±3%.

entry	sunscreen system in base cream {[%(w/w)], form}	synthetic sunscreen active / tannin (w/w)	UV range [a] [nm]	lowest transmission in UV region [b] [%]	λ (min. transmission) [b] [nm]
1	--- (*i.e.*, pure base cream)	---	A	---	---
		---	B	---	---
2	**olive oil**	1/0	A	100	325
	{5%, neat}		B	100	319
3	***Sb*T**	0/1	A	24	321
	{2%, neat}		B	39	290
4	**SLC**	1/0	A	---	---
	{10%, neat}		B	12	312
5	**BNZ + SLC**	1/0	A	29	349
	{15% (w/w) **BNZ** in **SLC** }		B	11	310
6	***Sb*T + SLC**	1/5	A	---	---
	{2% + 10%, each neat}		B	5	309
7	***Sb*T-MCs**	1/0	A	103	321
	{10%, neat O.O.}		B	101	290
8	**SLC@*Sb*T-MCs**	1/5	A	77	311
	{10%, 0.1% (w/w) **SLC** in O.O.}		B	77	365
9	**SLC@*Sb*T-MC**	100/1	A	32	321
	{10%, 50% (v/v) **SLC** in O.O.}		B	24	305
10	**SLC@*Sb*T-MC**	200/1	A	5	321
	{10%, neat **SLC**}		B	2	305
11	**BNZ/SLC@*Sb*T-MC**	200/1	A	29	349
	{10%, (15% (w/w) **BNZ** in **SLC**)}		B	11	310

a: UV-A range: 320-400 nm; UV-B range: 290-320 nm.

b: Average of three measurements; normalised data.

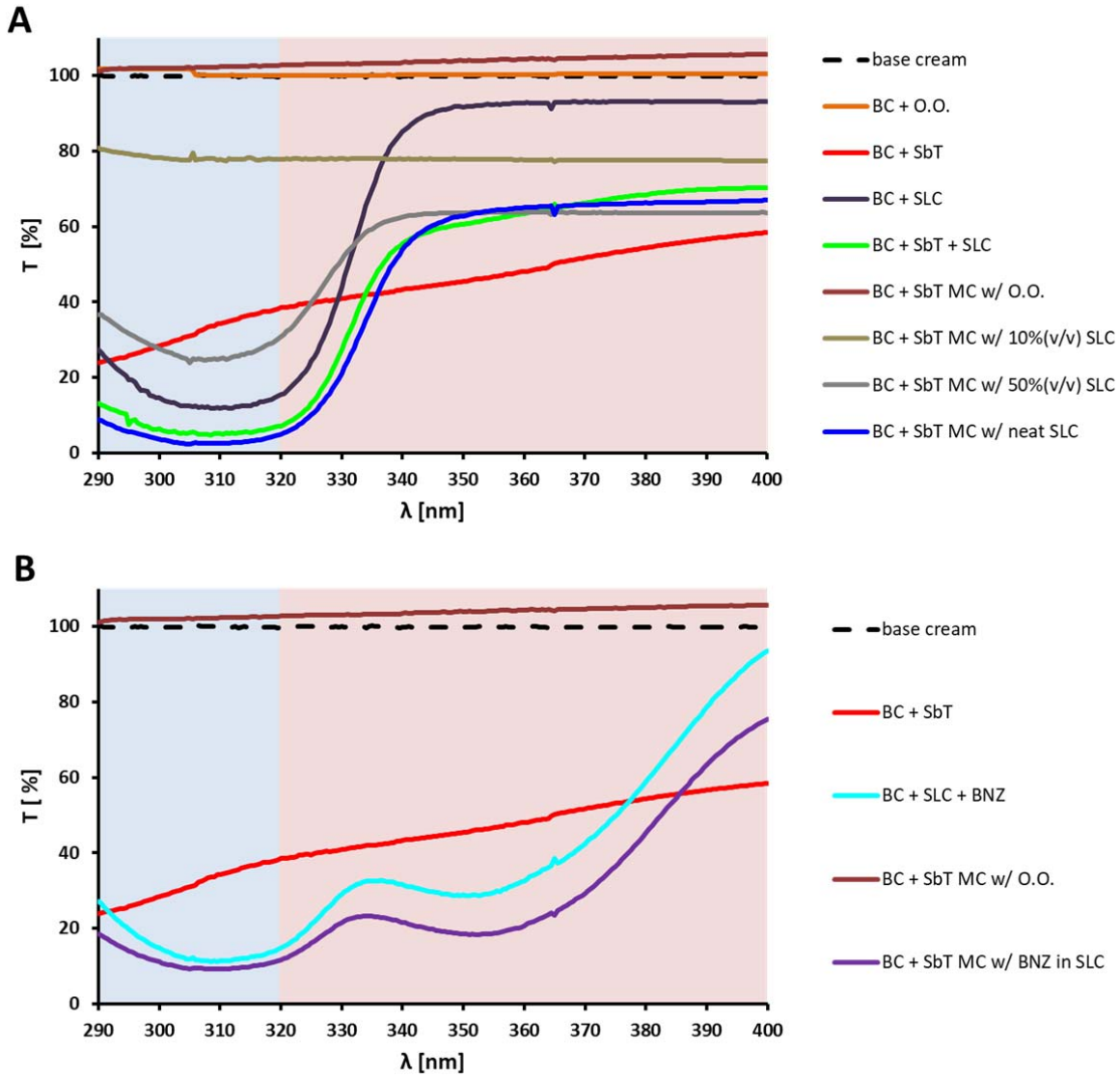

Figure 4. Comparisons of transmission spectra of base cream against sun cream preparations containing: (A) UV-B range systems (*i.e.*, **SLC** systems); (B) UV-A and UV-B range systems (*i.e.*, **SLC** & **BNZ** systems). Legend: BC, base cream; O.O., olive oil; *Sb*T, *Schinopsis balansae* tannin; **SLC**, 2-ethylhexyl salicylate; *Sb*T MC, *Sb*T microcapsules; **BNZ**, hexyl-2-[3-(diethylamino)-2-hydroxybenzoyl] benzoate.

Transmittance measurements of a sample consisting of pure base cream and cream with 5% olive oil did not show any reduction in trasmittance (Table 3, entries 1 and 2, Figure 4A). The same is observed when mixing in olive oil-containing ***Sb*T MCs** (Table 3, entry 7, Figure 4A); reduction

of the level at which this steady decline occurs fits the fact that the very thin ***Sb*T** shell of the capsules does not even lead to an overall tannin content of 2% (w/w) when adding 20% (w/w) capsules. This finding can be seen as an indirect conformation of earlier studies that indicated surprisingly fine shells in tannin capsules (Bartzoka et al., 2017). A cream sample containing 2% (w/w) ***Sb*T** in non-capsule form lead correspondingly to a gentle reduction in transmittance in both the UV-A and UV-B region (Table 3, entry 3, Figure 4A); in this case, no specific interaction in the sense of a peaking wave length is observed, but a rather steady gradual reduction in transmission.

A clear transmittance reduction to 12% in the UV-B region is seen for a sample containing 10% (w/w) **SLC** with respect to the mass of the base cream resulted in (Table 3, entry 4, Figure 4A). When evaluating the UV transmittance of sunscreen cream samples containing a mix of both **SLC** and ***SbT***, *i.e.*, the synthetic sunscreen not in capsule form in the presence of a smaller quantity of tannin (Table 3, entry 6, Figure 4A), the obtained transmittance spectrum suggests the expected synergistic effect of the two components: in the UV-A region, the tannin presence leads to a slight decrease in transmission, whereas **SLC** leads to a further decreased transmission value of 5% in the UV-B region.

When comparing base cream preparations comprising 10% (w/w) ***Sb*T MCs** filled with either 0.1%(w/w) **SLC** in olive oil, 50% (w/w) **SLC** in olive oil or neat **SLC** (Table 3, entries 8, 9 and 10, respectively, Figure 4A), comparable performances between the cream prepared with ***Sb*T**-MCs filled with neat **SLC** and cream containing ***Sb*T** and **SLC** as simple mix in the UV-B region, with the capsule-containing sample performing slightly but significantly better (Table 3, entries 6 and 10, respectively, Figure 4A), presumably due to a combination of synergistic effects and presence of capsulate material. Over the range of wavelengths of the UV-A region, performances of the two samples are essentially identical.

In light of the observed concentration effects, in order to have an effect also in the UV-A range, another type of ***Sb*T MCs** were designed that contain two synthetic sunscreen actives: UV-

A-targeting hexyl-2-[3-(diethylamino)-2-hydroxybenzoyl] benzoate (**BNZ**) and, as before, UV-B-targeting 2-ethylhexyl salicylate (**SLC**) (Table 2, entry 9. These capsules, exhibiting practically indistinguishable morphological characteristics, were mixed into the base cream used before at a concentration of 10% (w/w). Transmittance measurements led to the expected double UV-protection of the cream preparation (Table 3, entry 11, Figure 3B). More importantly, when comparing the transmittance curve of the capsule-based **BNZ**/**SLC** system (Table 3, entry 11), with the one obtained for the simple mix of **BNZ**/**SLC** in base cream (Table 3, entry 5), a beneficial synergistic effect of the tannin presence is again observed: the ***Sb*T** presence leads to an extended protection in the region between 310 and 290 nm. The synergistic effect is even more pronounced in the UV-A-region for the **BNZ** component.

4. Conclusions

Two novel synergy-enhanced sunscreen systems were presented, based on tannin-microcapsules filled with synthetic sunscreen agents: a system targeting solely the UV-B range, employing tannin microcapsules filled with neat 2-ethylhexyl salicylate (**SLC**), and one system targeting both the UV-A and the UV-B region comprising TMCs filled with **SLC** in which has been dissolved hexyl-2-[3-(diethylamino)-2-hydroxybenzoyl] benzoate (**BNZ**). The use of tannin capsules in these systems guarantees a double beneficial effect: tannin presence as such serves to extend the effective protection range of the UV-actives, especially in the UV-B range towards shorter and even more damaging wavelengths. By enhancing the effectivity of synthetic sunscreens *via* synergistic effects helps reducing the amount of synthetic sunscreens needed, and does thus contribute to the development of more sustainable and environmentally benign UV-protection systems. The demonstrated slow release of the sunscreen actives from the capsules serve further to maintain a protective function over a longer period of time, additionally enhanced by the fact that

the tannin protects the sunscreen from oxidative degradation. The intrinsic anti-inflammatory aspect of the tannin component does further represent a positive effect of the tannin presence in such sun-screen systems.

Funding

No dedicated funding to declare.

CRediT authorship contribution statement

Elisabetta Alfonsi: Investigation, Initial data analyses. **Heiko Lange:** Conceptualization, Methodology, Supervision, Data curation, Writing - Original draft preparation, Writing - Reviewing and Editing. **Crestini Crestini:** Conceptualization, Methodology, Funding, Data curation, Supervision, Writing- Reviewing and Editing.

Data availability

Data will be made available upon request.

Acknowledgements

The authors would like to thank Figli di Guido Lapi s.p.a. for providing *Schinopsis balansae* wood

extract and *Acacia mearnsii* bark extract. H.L. acknowledges the MIUR Grant 'Dipartimento di Eccellenza 2018-2022' to the Department of Earth and Environmental Sciences of the University of Milano-Bicocca. C.C acknowledges the Ca'Foscari FPI 2019 funding.

Conflict of interest statement

The authors declare that they have no known competing financial interests or personal relationships that could have appeared to influence the work reported in this paper.

Appendix A. Supporting Information

Supplementary data associated with this article, *i.e.*, figures detailing optical micrographs of the different capsule systems, release profiles, microscope-assisted stability studies, preparation of transmission measurements of sunscreen cream preparations, comparison of transmission spectra, can be found in the online version at doi:10.1016/j.indcrop.12345

References

Bartzoka, E.D., Lange, H., Mosesso, P., Crestini, C., 2017. Synthesis of nano- and microstructures from proanthocyanidins, tannic acid and epigallocatechin-3-O-gallate for active delivery. Green Chem. 19, 5074–5091. https://doi.org/10.1039/C7GC02009K

Bartzoka, E.D., Lange, H., Poce, G., Crestini, C., 2018. Stimuli-Responsive Tannin–FeIII Hybrid Microcapsules Demonstrated by the Active Release of an Anti-Tuberculosis Agent. ChemSusChem 11, 3975–3991. https://doi.org/10.1002/cssc.201801546

Bartzoka, E.D., Lange, H., Thiel, K., Crestini, C., 2016. Coordination Complexes and One-Step Assembly of Lignin for Versatile Nanocapsule Engineering. ACS Sustain. Chem. Eng. 4, 5194–5203. https://doi.org/10.1021/acssuschemeng.6b00904

Burnett, M.E., Wang, S.Q., 2011. Current sunscreen controversies: a critical review. Photodermatol. Photoimmunol. Photomed. 27, 58–67. https://doi.org/10.1111/j.1600-0781.2011.00557.x
Crestini, C., Lange, H., Bianchetti, G., 2016. Detailed Chemical Composition of Condensed Tannins via Quantitative 31P NMR and HSQC Analyses: Acacia catechu, Schinopsis balansae, and Acacia mearnsii. J. Nat. Prod. 79, 2287–2295. https://doi.org/10.1021/acs.jnatprod.6b00380
Donglikar, M., Deore, S., Deore, S., Deore, S., 2016. Sunscreens: A review. Pharmacogn. J. 8, 171–179. https://doi.org/10.5530/pj.2016.3.1
Gasparro, F.P., Mitchnick, M., Nash, J.F., 1998. A Review of Sunscreen Safety and Efficacy. Photochem. Photobiol. 68, 243–256. https://doi.org/10.1111/j.1751-1097.1998.tb09677.x
Gordobil, O., Olaizola, P., Banales, J.M., Labidi, J., 2020. Lignins from Agroindustrial by-Products as Natural Ingredients for Cosmetics: Chemical Structure and In Vitro Sunscreen and Cytotoxic Activities. Molecules 25, 1131. https://doi.org/10.3390/molecules25051131
Ibrahim, M.N.M., Iqbal, A., Shen, C.C., Bhawani, S.A., Adam, F., 2019. Synthesis of lignin based composites of TiO2 for potential application as radical scavengers in sunscreen formulation. BMC Chem. 13, 17. https://doi.org/10.1186/s13065-019-0537-3
Ichihashi, M., Ueda, M., Budiyanto, A., Bito, T., Oka, M., Fukunaga, M., Tsuru, K., Horikawa, T., 2003. UV-induced skin damage. Toxicology, Environmental and Nutritional Interactions Antioxidant Nutrients and Environmental Health, Part C 189, 21–39. https://doi.org/10.1016/S0300-483X(03)00150-1
Jiménez Reinosa, J., Leret, P., Álvarez-Docio, C.M., del Campo, A., Fernández, J.F., 2016. Enhancement of UV absorption behavior in ZnO–TiO2 composites. Bol. Soc. Esp. Cerámica Vidr. 55, 55–62. https://doi.org/10.1016/j.bsecv.2016.01.004
Khanbabaee, K., Ree, T. van, 2001. Tannins: Classification and Definition. Nat. Prod. Rep. 18, 641–649. https://doi.org/10.1039/B101061L
Kim, S., Choi, K., 2014. Occurrences, toxicities, and ecological risks of benzophenone-3, a common component of organic sunscreen products: A mini-review. Environ. Int. 70, 143–157. https://doi.org/10.1016/j.envint.2014.05.015
Kollias, N., 1999. The Absorption Properties of Physical Sunscreens. Arch. Dermatol. 135, 209-a-210. https://doi.org/10-1001/pubs.Arch Dermatol.-ISSN-0003-987x-135-2-dlt0299
Lapidot, N., Gans, O., Biagini, F., Sosonkin, L., Rottman, C., 2003. Advanced Sunscreens: UV Absorbers Encapsulated in Sol-Gel Glass Microcapsules. J. Sol-Gel Sci. Technol. 26, 67–72. https://doi.org/10.1023/A:1020785217895
Lee, S.C., Tran, T.M.T., Choi, J.W., Won, K., 2019. Lignin for white natural sunscreens. Int. J. Biol. Macromol. 122, 549–554. https://doi.org/10.1016/j.ijbiomac.2018.10.184
Lee, S.C., Yoo, E., Lee, S.H., Won, K., 2020. Preparation and Application of Light-Colored Lignin Nanoparticles for Broad-Spectrum Sunscreens. Polymers 12, 699. https://doi.org/10.3390/polym12030699
Li, Y., Yang, D., Lu, S., Qiu, X., Qian, Y., Li, P., 2019. Encapsulating TiO2 in Lignin-Based Colloidal Spheres for High Sunscreen Performance and Weak Photocatalytic Activity. ACS Sustain. Chem. Eng. 7, 6234–6242. https://doi.org/10.1021/acssuschemeng.8b06607
Masui, T., Hirai, H., Imanaka, N., Adachi, G., 2006. New sunscreen materials based on amorphous cerium and titanium phosphate. J. Alloys Compd., Proceedings of Rare Earths'04 in Nara, Japan 408–412, 1141–1144. https://doi.org/10.1016/j.jallcom.2004.12.136
More, B.D., 2007. Physical sunscreens: On the comeback trail. Indian J. Dermatol. Venereol. Leprol. 73, 80. https://doi.org/10.4103/0378-6323.31890
Mueller-Harvey, I., 2001. Analysis of hydrolysable tannins. Anim. Feed Sci. Technol., Tannins:Analysis and Biological Effects in Ruminant Feeds 91, 3–20. https://doi.org/10.1016/S0377-8401(01)00227-9
Narla, S., W. Lim, H., 2020. Sunscreen: FDA regulation, and environmental and health impact. Photochem. Photobiol. Sci. 19, 66–70. https://doi.org/10.1039/C9PP00366E

Pal, A., Hadagalli, K., Bhat, P., Goel, V., Mandal, S., 2020. Hydroxyapatite—a promising sunscreen filter. J. Aust. Ceram. Soc. 56, 345–351. https://doi.org/10.1007/s41779-019-00354-2

Patel, N.P., Highton, A., Moy, R.L., 1992. Properties of Topical Sunscreen Formulations: A Review. J. Dermatol. Surg. Oncol. 18, 316–320. https://doi.org/10.1111/j.1524-4725.1992.tb03677.x

Petersen, B., Wulf, H.C., 2014. Application of sunscreen − theory and reality. Photodermatol. Photoimmunol. Photomed. 30, 96–101. https://doi.org/10.1111/phpp.12099

Pfeifer, G.P., 2020. Mechanisms of UV-induced mutations and skin cancer. Genome Instab. Dis. 1, 99–113. https://doi.org/10.1007/s42764-020-00009-8

Piombino, C., Lange, H., Sabuzi, F., Galloni, P., Conte, V., Crestini, C., 2020. Lignosulfonate Microcapsules for Delivery and Controlled Release of Thymol and Derivatives. Molecules 25, 866. https://doi.org/10.3390/molecules25040866

Pizzi, A., 2008. Chapter 8 - Tannins: Major Sources, Properties and Applications, in: Belgacem, M.N., Gandini, A. (Eds.), Monomers, Polymers and Composites from Renewable Resources. Elsevier, Amsterdam, pp. 179–199. https://doi.org/10.1016/B978-0-08-045316-3.00008-9

Qian, Y., Qiu, X., Zhu, S., 2014. Lignin: a nature-inspired sun blocker for broad-spectrum sunscreens. Green Chem. 17, 320–324. https://doi.org/10.1039/C4GC01333F

Qian, Y., Zhong, X., Li, Y., Qiu, X., 2017. Fabrication of uniform lignin colloidal spheres for developing natural broad-spectrum sunscreens with high sun protection factor. Ind. Crops Prod. 101, 54–60. https://doi.org/10.1016/j.indcrop.2017.03.001

Qiu, X., Li, Y., Qian, Y., Wang, J., Zhu, S., 2018. Long-Acting and Safe Sunscreens with Ultrahigh Sun Protection Factor via Natural Lignin Encapsulation and Synergy. ACS Appl. Bio Mater. acsabm.8b00138. https://doi.org/10.1021/acsabm.8b00138

Sánchez-Quiles, D., Blasco, J., Tovar-Sánchez, A., 2020. Sunscreen Components Are a New Environmental Concern in Coastal Waters: An Overview. Springer, Berlin, Heidelberg, pp. 1–14.

Scheuer, E., Warshaw, E., 2006. Sunscreen Allergy: A Review of Epidemiology, Clinical Characteristics, and Responsible Allergens. Dermatitis 17, 3–11. https://doi.org/10.2310/6620.2006.05017

Schneider, S.L., Lim, H.W., 2019. Review of environmental effects of oxybenzone and other sunscreen active ingredients. J. Am. Acad. Dermatol. 80, 266–271. https://doi.org/10.1016/j.jaad.2018.06.033

Soehnge, H., Ouhtit, A., Ananthaswamy, O.N., 1997. Mechanisms of induction of skin cancer by UV radiation. Front. Biosci. J. Virtual Libr. 2, d538-551. https://doi.org/10.2741/a211

Suh, S., Pham, C., Smith, J., Mesinkovska, N.A., 2020. The banned sunscreen ingredients and their impact on human health: a systematic review. Int. J. Dermatol. 59, 1033–1042. https://doi.org/10.1111/ijd.14824

Thomas, M.L.R.M.G., Filho, J.M.B., 1985. Anti-inflammatory actions of tannins isolated from the bark of Anacardwm occidentale L. J. Ethnopharmacol. 13, 289–300. https://doi.org/10.1016/0378-8741(85)90074-1

Urbach, F., 2001. The historical aspects of sunscreens. J. Photochem. Photobiol. B, ESP Conference on Photoprotection 64, 99–104. https://doi.org/10.1016/S1011-1344(01)00202-0

Vanholme, R., Demedts, B., Morreel, K., Ralph, J., Boerjan, W., 2010. Lignin Biosynthesis and Structure. Plant Physiol. 153, 895–905. https://doi.org/10.1104/pp.110.155119

Zhang, H., Chen, F., Liu, X., Fu, S., 2018. Micromorphology Influence on the Color Performance of Lignin and Its Application in Guiding the Preparation of Light-colored Lignin Sunscreen. ACS Sustain. Chem. Eng. 6, 12532–12540. https://doi.org/10.1021/acssuschemeng.8b03464

Zhang, H., Liu, X., Fu, S., Chen, Y., 2019. High-value utilization of kraft lignin: Color reduction and evaluation as sunscreen ingredient. Int. J. Biol. Macromol. 133, 86–92. https://doi.org/10.1016/j.ijbiomac.2019.04.092

Zhen, L., Lange, H., Crestini, C., 2021. An Analytical Toolbox for Fast and Straightforward Structural Characterisation of Commercially Available Tannins. Molecules 26, 2532. https://doi.org/10.3390/molecules26092532

Graphical abstract